IEEE Access
Multidisciplinary ⋮ Rapid Review ⋮ Open Access Journal

Received August 1, 2017, accepted August 18, 2017, date of publication August 24, 2017, date of current version September 19, 2017.

Digital Object Identifier 10.1109/ACCESS.2017.2744498

A Symmetrical Hybrid Driving Waveform for a Linear Piezoelectric Stick-Slip Actuator

HENGYU LI[1], YIKANG LI[1], TINGHAI CHENG[1], XIAOHUI LU[1], HONGWEI ZHAO[2], AND HAIBO GAO[3]

[1]Mechatronic Engineering Department, Changchun University of Technology, Changchun 130012, China
[2]Department of Mechanical Science and Engineering, Jilin University, Changchun 130025, China
[3]State Key Laboratory of Robotics and System, Harbin Institute of Technology, Harbin 150001, China

Corresponding authors: Tinghai Cheng (chengtinghai@163.com) and Haibo Gao (gaohaibo@hit.edu.cn)

This work was supported in part by the Technology Research Planning Project of Education Department of Jilin Province under Grant 2016332, in part by the Jilin Province Science and Technology Development Plan Item under Grant 20150312006ZG, in part by the Key Projects of Science and Technology Development Plan of Jilin Province under Grant 20160204054GX, and in part by the State Key Laboratory of Robotics and System, Harbin Institute of Technology and Science, under Grant SKLRS-2016-KF-14.

ABSTRACT A symmetrical hybrid driving waveform (SHDW) is proposed in this paper, which includes a symmetrical saw-tooth driving waveform and a sinusoidal friction regulation waveform, and the sinusoidal friction regulation waveform is applied to the shrinkage period of the symmetrical saw-tooth driving waveform. In other words, the proposed SHDW can be achieved when the waveform symmetry of the hybrid driving method is 50%. The SHDW can effectively drive the designed symmetrical linear piezoelectric stick-slip actuator, and the motion direction is also easily regulated. The excitation principle of the actuator excited by the SHDW is explained in detail. A prototype is fabricated and the experimental investigations of the actuator characteristics are carried on. The higher velocity and the larger driving capacity are realized using by the SHDW relative to the asymmetrical hybrid driving waveform. Testing results show that the prototype excited by the SHDW can obtain the peak no-load speeds of 0.41 and 0.39 mm/s in the forward and reverse directions when the saw-tooth driving waveform voltage is 10 $V_{p\text{-}p}$ for 800 Hz and the sinusoidal friction regulation waveform voltage is 2 $V_{p\text{-}p}$ for 39 kHz. The step efficiencies can reach 92% and 90%. The driving capacities can reach 10.52 and 9.85 [(mm/s)g/mW] with the load of 70 g under the locking force of 0.1 N. The actuator excited by the SHDW will make it ideal for miniature information technology devices.

INDEX TERMS Stick-slip actuator, symmetrical hybrid driving waveform, symmetry, hybrid driving method.

I. INTRODUCTION

Piezoelectric stick-slip actuators have become viable candidates for miniature information technology devices of camera focusing mechanisms, cell phones, scanning probe microscopes, zoom lens systems, and blue-ray devices [1]–[3], due to the compact structure, low production cost, theoretically unlimited displacement, and the convenient control [4]–[7]. It is well known that the actuators make use of the inertia of the driven part to drive it in a small step through the uninterrupted friction contact, and the similar saw-shaped displacement can be obtained based on inverse piezoelectric effect [8]–[10]. The appropriate signal is conducive to the driving characteristics and proper operation of the stick-slip actuators [11]–[14].

The asymmetrical driving signals are generally used to drive the piezoelectric stick-slip actuators, aiming at obtaining the similar saw-shaped displacements. Yang *et al.* researched the stepping motion of a piezoelectric device based on triangular waveforms, and the impulse model is proposed to describe the motion behavior. Although the results validate the efficacy of the proposed model, not all inputs of the symmetries can make the actuator work well [15]. Yoshida *et al.*[16] proposed the smooth impact drive mechanism that can be modified the construction of the impact drive mechanism. The actuator excited by the rectangular waveform can be driven to generate the similar saw-shaped displacement and can achieve a high positioning resolution and a long stroke. Peng *et al.* [17] proposed a linear piezoelectric stick-slip actuator for the precision positioning of dual objects based on a double friction drive principle, which is excited by the saw-tooth driving waveform. The actuator has the potential to be constructed compactly. However,

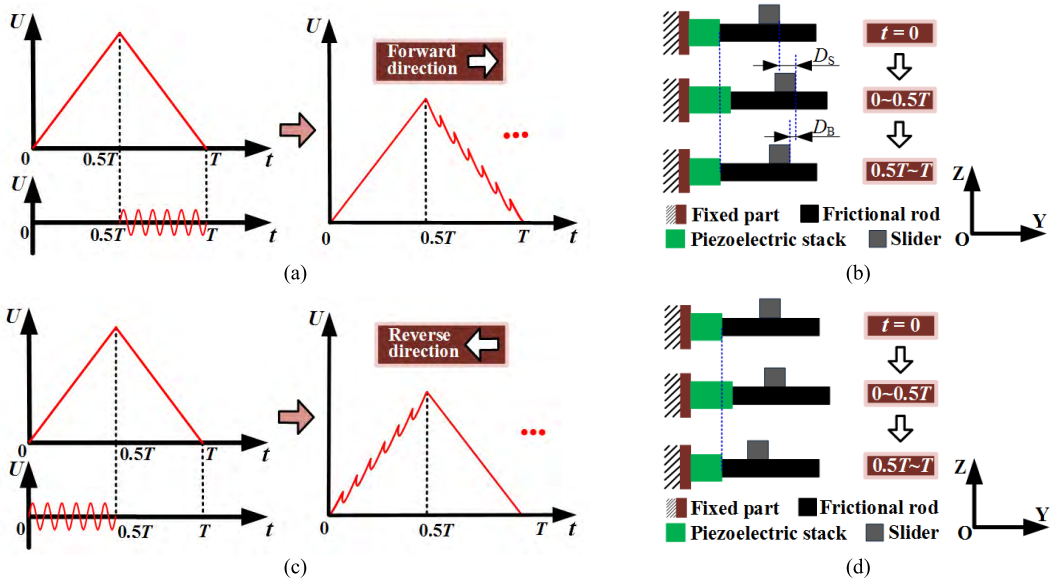

FIGURE 1. Exciting principle of the designed actuator using the SHDW. (a) Waveform schematic in the forward direction. (b) Operation process in the forward direction. (c) Waveform schematic in the reverse direction. (d) Operation process in the reverse direction.

the output velocity of the actuator is approximately zero when the input symmetry of the saw-tooth driving waveform was from 45% to 55%. Ma *et al*. [18] developed a resonant-type inertial impact actuator excited by the rectangular pulse. The actuator features a simple mechanical and an electrical design, which makes it ideal for miniature information technology device. It need to be noted that the actuator cannot move with waveform symmetry near 50% because no obvious similar saw-shaped displacement was output. Besides, the study on the cycloidal waveform has also been reported, which is used to drive the symmetrical stick-slip actuator [19]–[21]. This waveform merit is that the stick-slip motion is able of moving small objects against gravity. This contributes to the realization of the multi-freedom devices with compact design, and the design itself is easily miniaturized, which leads to the very stable instruments, especially for the scanning microscope applications. But these devices excited by the cycloidal waveform perform the undesirable characteristics than saw-tooth like waveform, both for the motion threshold and for the consistency of the step size [22], [23].

In our previous work, a hybrid driving method (HDM) for the stick-slip actuator has been proposed, which can be realized by the composite waveform. The composite waveform consists of the saw-tooth driving waveform and the sinusoidal friction regulation waveform which is applied to the rapid deformation stage of the saw-tooth driving waveform, aiming at decreasing the kinetic frictional force in the rapid deformation stage based on ultrasonic friction reduction. The investigations indicate that the previously proposed hybrid driving method (HDM) could effectively restrain the backward displacement, improving the low voltage characteristics, enhancing the load characteristics of the stick-slip actuator [24]–[26].

In this paper, the symmetrical hybrid driving waveform (SHDW) is proposed. The SHDW not only effectively drives the symmetrical linear piezoelectric stick-slip actuator, but also the motion direction is easily regulated, which effectively solves the traditional disadvantage that a symmetrical driving signal cannot drive the symmetrical linear stick-slip actuator. Besides, the influence of waveform symmetry based on the HDM on the output performance of the actuator is also further researched. This research work helps to provide an important guide for the practical applications of the stick-slip actuators excited by the SHDW. This paper is organized as follows: Section II describes the exciting principle of actuator excited by the SHDW. Section III shows the fabricated prototype in detail. Section IV shows that the experimental system. Section V states that a series of experiments are carried out to study the actuator characteristics. Finally, the section VI concludes this paper and indicates the future research work.

II. EXCITING PRINCIPLE

Fig. 1 shows the exciting principle of the symmetrical linear stick-slip actuator excited by the SHDW based on the HDM. The HDM includes the saw-tooth driving waveform and the sinusoidal friction regulation waveform [24]–[26]. The SHDW shown in Fig. 1(a) is applied to drive the actuator. A complete driving cycle of the actuator seen in Fig. 1(b) is explained in detail. Firstly, the piezoelectric stack is in natural length state and no voltage is applied on it. The slider and the frictional rod are in static state, such as the period of $t = 0$. Secondly, the piezoelectric stack extends, and the slider can move forward a distance along to the Y positive direction together with the frictional rod because of friction force. A driving displacement D_S is obtained in the expansion period of 0-0.5T. Finally, the piezoelectric stack

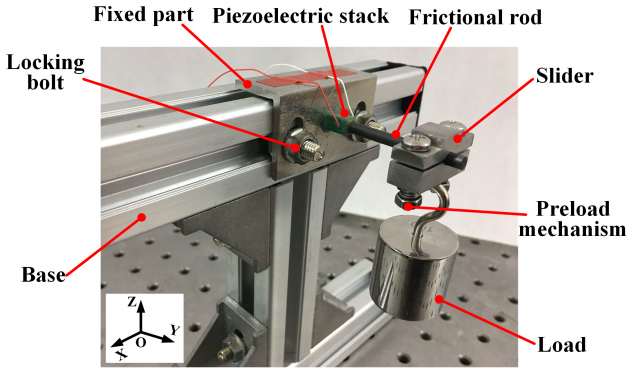

FIGURE 2. Photograph of the designed prototype.

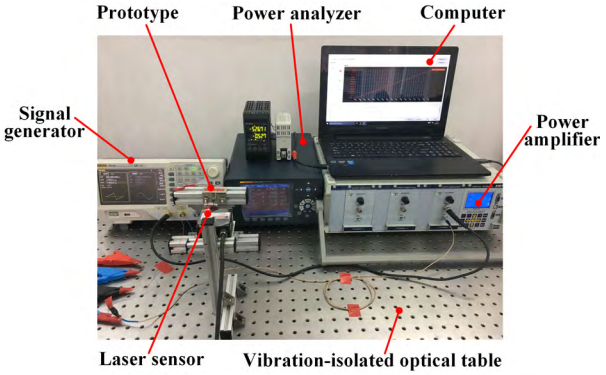

FIGURE 3. Photograph of the established experimental system.

returns back to the original position. The slider moves back a distance along to the Y negative direction together with frictional rod, and the backward displacement D_B is generated in the shrinkage period of $0.5T$-T. Above all, in shrinkage period, the resonant sinusoidal friction regulation waveform can excite the stator to generate a micro vibration with high frequency. The smaller friction force between the frictional rod and slider is obtained relative to the expansion period. The smaller backward displacement D_B is generated relative to the driving displacement D_S. Therefore, the larger effective step displacement ΔD_S of the stick-slip actuator can be obtained. The continuous motion can be achieved by using the periodic symmetrical hybrid driving waveform (SHDW). Reversible slider motion is possible by applying the resonant sinusoidal friction regulation waveform to expansion period of symmetrical saw-tooth driving waveform, as shown in Fig. 1(c) and (d).

III. FABRICATION OF PROTOTYPE

Fig. 2 shows that the designed prototype of the symmetrical linear piezoelectric stick-slip actuator, which consists of a piezoelectric stack (AE0505D08F, NEC-Tokin Corporation, Japan), a frictional rod, a slider, a fixed part, a base, a preload mechanism, two locking bolts, and the load. The frictional rod is fixed to the piezoelectric stack by expoxy resin adhesive. The Carbon Fiber Reinforced Plastic (CFRP) is the selected material for the frictional rod because of the high stiffness and the low density. The diameter and the length of the frictional rod are ϕ4 mm and 40 mm, respectively. The piezoelectric stack is fixed on the fixed part through expoxy resin adhesive, and the section area and the length of piezoelectric stack are 5 mm×5 mm and 10 mm, respectively. The fixed part is made of the 304 stainless steel, and the fixed part is installed the base by the two locking bolts. The base is made of the aluminium alloy AL7075. The locking bolt is made of the 304 stainless steel. In addition, the piezoelectric stack and the frictional rod can constitute a stator, and the mass of the stator is 4 g. The schematic diagram of the prototype is shown in Fig. 7 in detail. The locking force of the stick-slip actuator is easily changed by adjusting the preload mechanism.

IV. EXPERIMENTAL SYSTEM

Fig. 3 shows the experimental system of the actuator, which includes a computer, a power analyzer (NORMA4000, Fluke Co. Ltd, America), a laser sensor (LK-H020, Keyence Co. Ltd, Japan), a power amplifier (XE500-C, Harbin Core Tomorrow Science & Technology Co. Ltd, China), a signal generator (DG4162, Beijing RIGOL Technology Co. Ltd, China), and a prototype. All of the experiment equipments are fixed on the vibration-isolated optical table. When the experimental system works, the signal generator controlled by the computer can be used to provide a wanted waveform, and the driving voltage range of the signal generator is from −10 V to +10 V. The driving voltage can be amplified by the power amplifier. The enlarged voltage is used to drive the prototype directly. The prototype can generate a continuous output motion by the periodic symmetrical hybrid driving waveform (SHDW). The laser sensor with the resolution of 20 nm is used to measure motion behavior of the actuator under different locking forces. It should be noted that the locking force is the largest load along to the axial direction of frictional rod that the mechanism can hold, and it is measured by hanging a load along the axial direction until the slider is just about to move. The locking force is a function of the preload force between the frictional rod and slider. The data are gathered by its built-in software via the computer. Meanwhile, the input power of the actuator can be tested by means of the power analyzer.

V. EXPERIMENTS AND RESULTS

The relationship between the driving frequency and output velocity with the initial slider mass of 30 g under the different locking forces is indicated in Fig. 4. Experimental results of the frequency characteristics indicate that the output velocity goes up while the frequency increases. When the symmetrical saw-tooth driving and sinusoidal friction regulation waveform voltages are 10 $V_{p\text{-}p}$ at 800 Hz and 2 $V_{p\text{-}p}$ at 39 kHz, the output velocities in the forward direction can reach 0.30 mm/s under the locking force of 0.2 N; the output velocities are 0.19 mm/s under the locking force of 0.3 N. Compared with the locking forces of 0.2 N and

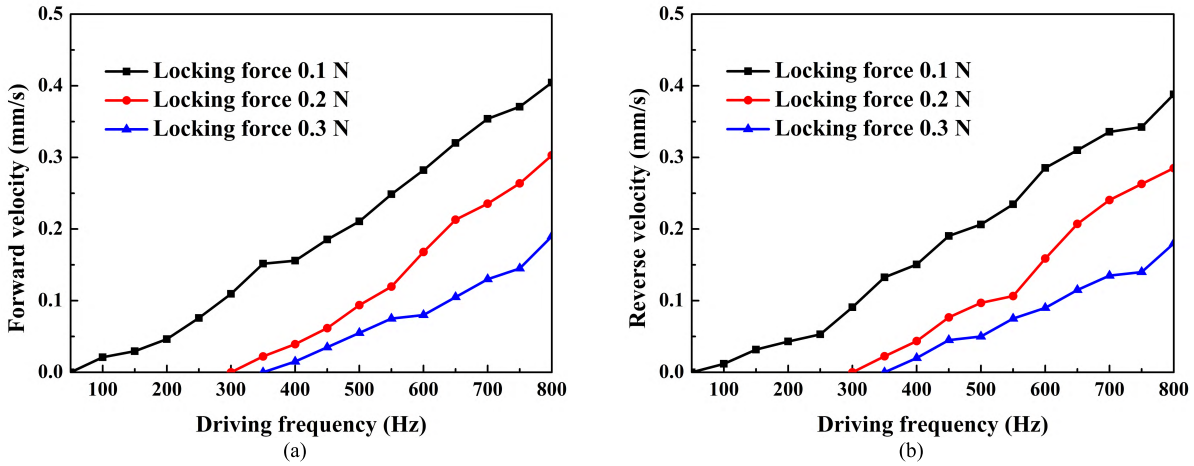

FIGURE 4. Velocity versus to the driving frequency with an initial mass of the slider of 30 g. (a) Forward velocity under the different locking forces. (b) Reverse velocity under the different locking forces.

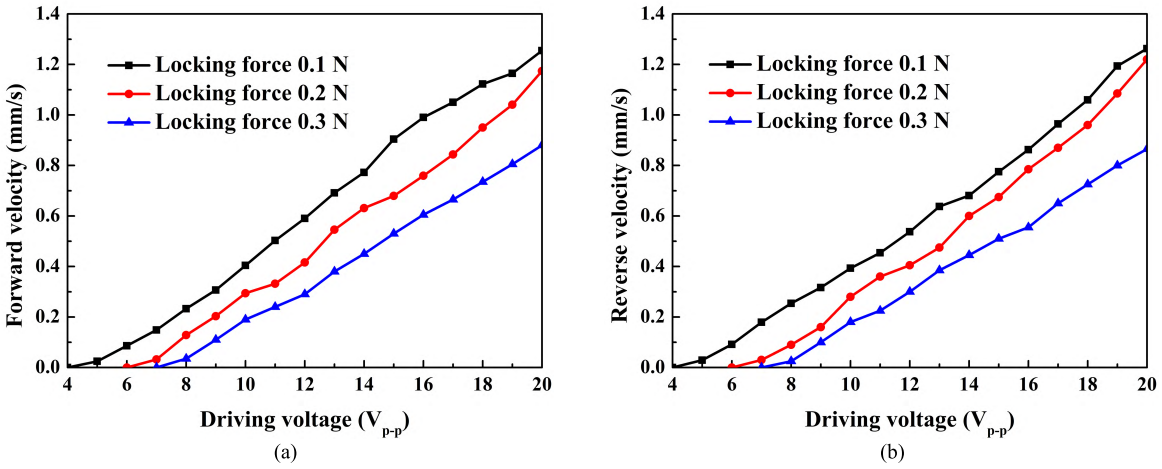

FIGURE 5. Velocity versus to the driving voltage with an initial mass of the slider of 30 g. (a) Forward velocity under the different locking forces. (b) Reverse velocity under the different locking forces.

0.3 N, the higher velocity of 0.41 mm/s is obtained under the locking force of 0.1 N. The locking force has an influence on the velocity characteristic, as shown in Fig. 4(a). The similar velocity characteristic can be realized in the reverse direction, seen in Fig. 4(b). The designed symmetrical linear stick-slip actuator is driven by the SHDW, and the motion direction can be easily regulated in this paper, as shown in Fig.1 (a) and Fig. 1(c). Besides, the minimum driving frequencies are 50 Hz, 300 Hz and 350 Hz when the locking forces are 0.1 N, 0.2 N and 0.3 N, respectively. It can be concluded that the symmetrical linear piezoelectric stick-slip actuators can easily achieve a lower frequency actuation under the small locking force. Here, it need to be pointed out that the relationship between the driving frequency and output velocity is not linear; this may be caused by the influence of preloading gap between the frictional rod and the slider and the assembly errors of the stator.

Fig. 5 gives the relationship between the driving voltage and output velocity with an initial mass of the slider of 30 g. The driving frequency of symmetrical saw-tooth driving waveform is 800 Hz and the voltage of the sinusoidal friction regulation waveform is 2 $V_{p\text{-}p}$ for 39 kHz. The output velocity of actuator excited by the SHDW increases linearly with driving voltage. The forward velocity under the locking force of 0.1 N reaches 0.41 mm/s when the voltage is 10 $V_{p\text{-}p}$; the velocity can reach 1.25 mm/s under the voltage of 20 $V_{p\text{-}p}$, as shown in Fig. 5(a). Meanwhile, the reverse velocity reaches 0.39 mm/s under the voltage of 10 $V_{p\text{-}p}$. The velocity can reach 1.26 mm/s under the voltage of 20 $V_{p\text{-}p}$, as shown in Fig. 5(b). The actuator excited by the SHDW has the better voltage characteristics. Although the output velocity approximately follows the linear increasing tendency with the increasing driving voltage, it is not an ideal straight line. This may be caused by a different actual contact position between the frictional rod and the slider. Besides, the minimum operation voltage of the actuator is 4 $V_{p\text{-}p}$ under the locking force of 0.1 N. Under the locking force of 0.2 N and 0.3 N, the minimum operation voltages are 6 $V_{p\text{-}p}$ and 7 $V_{p\text{-}p}$.

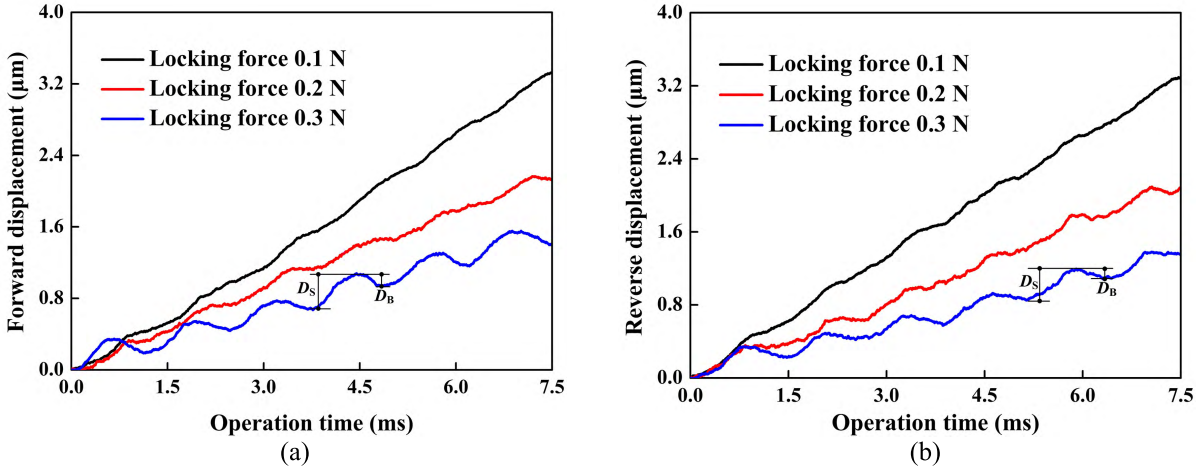

FIGURE 6. Displacement versus to the operation time with an initial mass of the slider of 30 g. (a) Forward displacement under the different locking forces. (b) Reverse displacement under the different locking forces.

The actuator excited by the SHDW can be easily driven at the low voltage and a stable operation can be easily obtained under the different locking forces. The actuator can obtain the better driving characteristics at low driving voltage, and the SHDW can make the actuator obtain the large voltage operation scope. Besides, the heat generation is significantly reduced because the dielectric losses are effectively suppressed operating at low voltage [27], [28].

It should be noted that the optimal voltage ratio between the sinusoidal friction regulation waveform and the symmetrical saw-tooth driving waveform is 0.2. Besides, the ideal driving characteristics of the actuator can be achieved at a resonant frequency of 39 kHz [26]. Based on this, the driving voltage and the driving frequency of symmetrical saw-tooth driving waveform are 10 $V_{p\text{-}p}$ and 800 Hz, and the driving voltage and the driving frequency of the sinusoidal friction regulation waveform are 2 $V_{p\text{-}p}$ and 39 kHz, which are selected for the following experiments.

Fig. 6 indicates the relationship between the operation time and the displacements under the different locking forces. The actuator excited by the SHDW can obtain a stable operation. Although the displacement curve appears an increased linear line, not is an ideal linear. A larger fluctuation of displacement is generated under a large locking force. This may be caused by the influence of the larger kinetic friction force between the frictional rod and the slider, and the elastic deformation of the frictional rod should also be considered.

An effective step displacement ΔD_S is introduced, and the effective step displacement ΔD_S is expressed as follows:

$$\Delta D_S = D_S - D_B \tag{1}$$

where D_S is the driving displacement, D_B is the backward displacement, ΔD_S is the effective step displacements. According to (1), the step efficiency η is shown as follows:

$$\eta = \frac{\Delta D_S}{D_S} \times 100\% \tag{2}$$

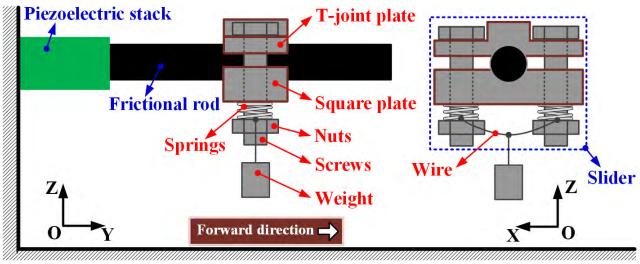

FIGURE 7. Working schematic of the vertical load experimental system.

TABLE 1. Tested results in the forward direction.

Locking force	Forward motion			
F (N)	D_S (μm)	D_B (μm)	ΔD_S (μm)	η (100%)
0.1	0.51	0.04	0.47	0.92
0.2	0.47	0.11	0.36	0.77
0.3	0.49	0.25	0.24	0.49

TABLE 2. Tested results in the reverse direction.

Locking force	Reverse motion			
F (N)	D_S (μm)	D_B (μm)	ΔD_S (μm)	η (100%)
0.1	0.50	0.05	0.45	0.90
0.2	0.48	0.13	0.35	0.72
0.3	0.48	0.22	0.26	0.54

Based on (1) and (2), a driving displacement and backward displacement are listed in Table 1 and 2. The effective step displacement of the actuator in the forward direction reaches 0.47 μm, and the maximum step efficiency is 92%, as shown in Fig. 6(a) and Table 1. On the contrary, the effective step displacements of the actuator can reach 0.45 μm, and the maximum step efficiency is 90%, as shown in Fig. 6(b) and Table 2. The designed actuator excited by the symmetrical hybrid driving waveform (SHDW) can easily obtain the large step efficiency in both directions.

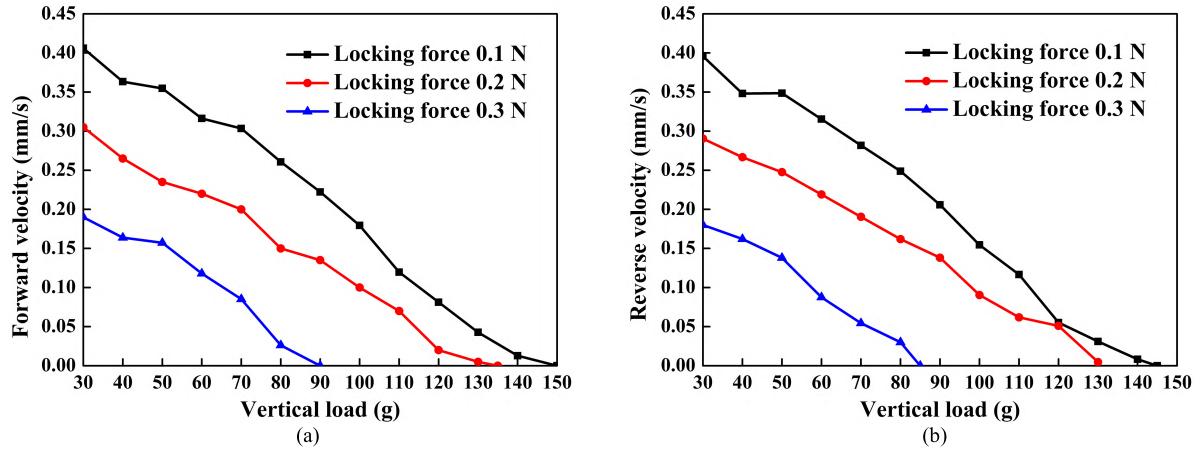

FIGURE 8. Velocity versus to the vertical load. (a) Forward velocity under the different locking forces. (b) Reverse velocity under the different locking forces.

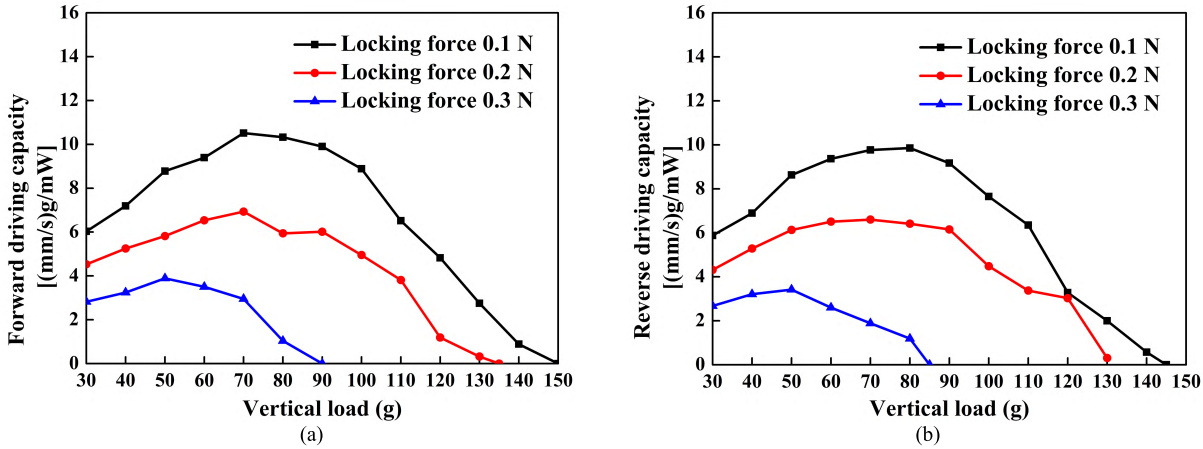

FIGURE 9. Driving capacity versus to the vertical load. (a) Forward driving capacity under the different locking forces. (b) Reverse driving capacity under the different locking forces.

During real actuator applications, the external vertical load of this type of actuator is an important factor, which obviously affects actuator performance. The vertical load experimental system of the actuator was used to measure the vertical load characteristics, which includes two screws, a T-joint plate, a square plate, two springs, two nuts and a wire. The photograph of the experimental system is shown in Fig. 2, and the detailed working schematic is shown in Fig. 7. Specifically, the T-joint plate and the square plate are fixed up by means of the thread matching of the screws and nuts, and the springs are inserted between the screws and the nuts. The wire is used to tow the vertical weight along to the Z positive direction. The vertical load of the actuator can be effectively changed by means of the wire tow the different weight. To investigate the influence of the external vertical load on the output performance of the actuator, the experimental test of the actuator is conducted at a given voltage of the symmetrical saw-tooth driving waveform of 10 $V_{p\text{-}p}$ for 800 Hz and the resonant sinusoidal friction regulation waveform of 2 $V_{p\text{-}p}$ for 39 kHz.

The standard weight is used to measure the vertical load of the actuator. The relationship between the vertical load and the output velocity under the different locking forces is shown in Fig. 8. The initial slider mass is 30 g without the external vertical load. During this experiment, the various weights were loaded on the slider along to Z negative direction by means of the wire, as shown in Fig. 7. The results indicate that the output velocity of the actuator decreases with the increased vertical load. The maximum vertical loads in the forward direction can reach 90 g, 135 g and 150 g under the locking forces of 0.1 N, 0.2 N and 0.3 N, respectively, seen in Fig. 8(a). Meanwhile, the maximum vertical loads in the reverse direction reach 85 g, 130 g and 145 g, respectively, seen in Fig. 8(b). In addition, an important parameter of mass ratio λ of the actuator is defined by as follows:

$$\lambda = \frac{M_{\max}}{M_S} \tag{3}$$

where $M_{\max}$ is the maximum vertical load under the different locking force, which can be obtained from the Fig. 8(a) and (b). M_S is the mass of the stator, which includes the frictional rod and the slider, and the net mass of the stator is 4 g. According to (3), the maximum mass ratios of the actuator in the forward and reverse directions are about 37:1 and 36:1.

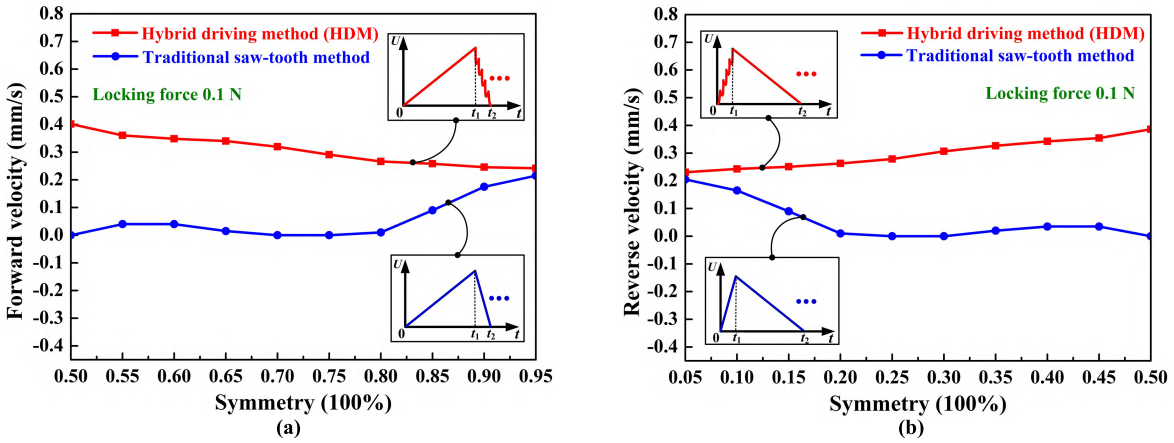

FIGURE 10. Velocity versus to the symmetry with an initial mass of the slider of 30 g. (a) Forward velocity under locking force of 0.1 N. (b) Reverse velocity under a locking force of 0.1 N.

This type of actuator is generally used to drive vertical load in the scanning probe microscopes, zoom lens systems, and camera lens modules. Basically, a tradeoff of velocity and vertical load should be considered depending on the different applications. Besides, a driving capacity is generally expected to be high for fitting into the mentioned miniature information devices. The driving capacity K [26], is introduced as follows:

$$K = \frac{M \times v}{P} \tag{4}$$

where M is the mass of the vertical load, v is the velocity under the different vertical load, P is the input power excited by the SHDW. The input power P of the actuator is 2.02 mW, which is measured by the power analyzer. The relationship between the vertical load and driving capacity of the actuator excited by the SHDW is shown in Fig. 9(a) and (b). The driving capacity increases with an increasing vertical load, and then it drops after the optimum vertical load. The large driving capacity is obtained under a locking force of 0.1 N. The driving capacities in the forward and reverse directions are 10.52 [(mm/s)g/mW] and 9.85 [(mm/s)g/mW] at the vertical load of 70 g.

The waveform symmetry (duty ratio) is also one of the key input parameters of the stick-slip actuator. The waveform symmetry in this paper is defined as follows:

$$S = \frac{t_1}{t_2} \times 100\% \tag{5}$$

where S is the symmetry based on the HDM, $0 \sim t_1$ is the time of the driving voltage going up, $0 \sim t_2$ is the time of a driving cycle. It need to be noted that the definition of symmetry is suitable for traditional saw-tooth method. The influence of waveform symmetry on the actuator characteristics is also further studied in this paper. The experiments of the velocity characteristics and load characteristics are carried out under a locking force of 0.1 N, which is chosen because the better performances and the more stable operation of the system are obtained, such as the generation of the higher velocity, smoother motion, and the larger driving capacity.

Fig. 10 indicates the relationship between the waveform symmetry and output velocity under the traditional saw-tooth driving method and the hybrid driving method (HDM) with an initial slider mass of 30 g. The parameters of the traditional saw-tooth driving method are the same as saw-tooth driving waveform of the HDM. The driving voltage and frequency are 10 $V_{p\text{-}p}$ and 800 Hz, respectively. For the traditional saw-tooth driving method, the actuator cannot work stably between the symmetry of 50%-80% and 20%-50%, because no obvious similar saw-shape displacement is output, especially for the symmetry of 50%. The larger velocity is obtained when the symmetries are 95% and 5%, and the velocities are 0.21 mm/s and 0.20 mm/s. The symmetry of traditional saw-tooth method in between 80%-95% and 5%-20% can only be used in the practical applications. On the contrary, the actuators excited by the HDM can obtain the higher velocity easier when the symmetries are 95% and 5%, the velocities are 0.24 mm/s and 0.23 mm/s, and the velocity has a linear increasing tendency in both between 95%-50% and 5%-50%. Here, it needs to be pointed out that the highest velocity can be realized by means of the symmetrical hybrid driving waveform (SHDW) relative to asymmetrical hybrid driving waveform, such as in between 95%-55% and 5%-45%, and the designed actuator excited by the SHDW can reach 0.41 mm/s and 0.39 mm/s in forward and reverse directions, respectively. The effective symmetry of the driving waveform based on the HDM is obviously widened relative to traditional saw-tooth driving method, especially for the SHDW proposed in this paper.

Fig. 11 shows the relationship between the vertical load and output velocity under the different input waveform symmetries, such as the symmetries of 90%, 70%, 50% (also known as the SHDW), 30%, and 10% in both directions. The results indicate that the output velocity decreases with the increasing vertical load. It can be seen that the actuator performs the ideal vertical load characteristics. The output velocity of the actuator excited by the waveform symmetries with 50%, 70%, and 90% is the almost similar when the vertical

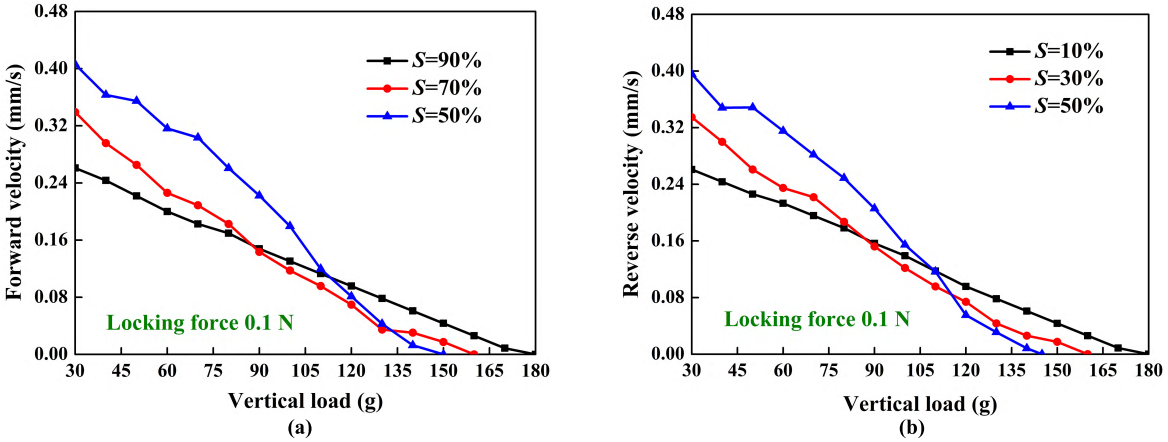

FIGURE 11. Velocity versus to the vertical load. (a) Forward velocity with the symmetries of 50%, 70% and 90%. (b) Reverse velocity with the symmetries of 10%, 30% and 50%.

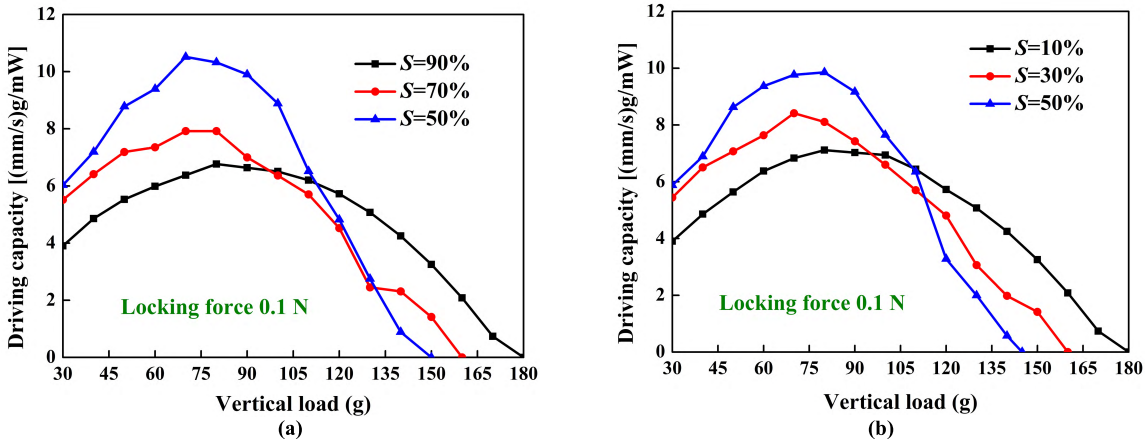

FIGURE 12. Driving capacity versus to the vertical load. (a) Forward driving capacity with the symmetries of 50%, 70% and 90%. (b) Reverse driving capacity with the symmetries of 10%, 30% and 50%.

load is 110 g. Before the vertical load of 110 g, the higher velocity is obtained when the symmetry is 50% under same vertical load. After the vertical load of 110 g, the higher velocity is obtained under 90%, and the maximum vertical load reaches 180 g, seen in Fig. 11(a). The asymmetrical hybrid driving waveform under 90% can achieve the better vertical load capacity when the voltage of the symmetrical saw-tooth driving waveform is 10 $V_{p\text{-}p}$ for 800 Hz and the sinusoidal friction regulation waveform is 2 $V_{p\text{-}p}$ for 39 kHz. The actuator in the reverse direction can achieved the similar load characteristics, as shown in Fig. 11(b). The larger stiffness is obtained under the symmetries of 90% and 10%. In addition, there is almost the same variation tendency of the vertical load characteristics in the forward and reverse directions.

The input powers of the actuator excited by the waveform symmetries of 50%, 70%, and 90% and the symmetries of 50%, 30%, and 10% are measured by the power analyzer. The input power under the symmetries of 50%, 70%, and 90% are 2.02 mW, 1.85 mW, and 2.01 mW, as shown in Table 3.

TABLE 3. Input power in the forward direction.

Waveform symmetry	90%	70%	50%
Input power (mW)	2.01	1.85	2.03

TABLE 4. Input power in the reverse direction.

Waveform symmetry	10%	30%	50%
Input power	2.02	1.84	2.03

The input power under 10%, 30%, and 50% are 2.01 mW, 1.84 mW, and 2.02 mW, as shown in Table 4.

According to the results of the Fig. 11, the driving capacity is calculated based on (4). The relationship between vertical load and driving capacity is shown as Fig. 12. The driving capacities reach 7.92 [(mm/s)g/mW] and 6.77 [(mm/s)g/mW] under the symmetries of 70% and 90%. The driving capacities under symmetries of 30% and 10% are 8.42 [(mm/s)g/mW] and 7.11 [(mm/s)g/mW]. Compared

with asymmetrical hybrid driving waveform, such as the symmetries of 90%, 70%, 30%, and 10%, the larger diving capacity of the actuator excited by the SHDW, such as the symmetry of 50%, can be easily realized before a vertical load of 110 g. The optimum vertical load in both directions is about 70 g. When the vertical load exceeds 150g, the smaller diving capacity excited by the SHDW will be obtained relative to the asymmetrical hybrid driving waveform. Comprehensive consideration of driving characteristics of actuator, the SHDW in this paper achieves better performance under certain conditions, such as the higher velocity, the larger driving capacity. In fact, it is surprising because the proposed SHDW has very blunt turning point for shrinkage period that follows and are not supposed to produce the larger inertial force for the sliding. The reason of the high velocity and large driving capacity is concluded as follows: On the one hand, the distortion of PZT displacement waveform with symmetry of 50% is not so serious as that at symmetries of 10%, 30%, 70% and 90%, which is owing to the creeping and hysteresis property of piezoelectric materials [23]. On the other hand, the locking force may have a vital influence on the driving characteristics of symmetrical driving system.

VI. CONCLUSIONS

This paper mainly presents the experimental characteristics of the symmetrical hybrid driving waveform (SHDW). The waveform schematic of the SHDW and the operation process were discussed in detail. The SHDW can drive a symmetrical stick-slip actuator, and the motion direction can be regulated relative to traditional symmetrical driving signals, such as the triangular waveform, the symmetrical rectangular pulse, the symmetrical saw-tooth driving waveform, and so on. The merit of the proposed SHDW is concluded as follows:

Firstly, the actuator excited by the SHDW can perform the higher output velocity, smoother motion, and larger driving capacity under a locking force of 0.1 N. The actuator in both directions achieves the peak no-load speeds of 0.41 mm/s and 0.39 mm/s. The minimum operation voltage is 4 $V_{p\text{-}p}$. The forward and reverse step efficiencies reach 92% and 90%, and the vertical loads reach 150 g and 145 g. The driving capacities can reach 10.52 [(mm/s)g/mW] and 9.85 [(mm/s)g/mW] at the vertical load of 70 g.

Secondly, the research on the waveform symmetry indicates that the effective waveform symmetry based on the HDM is widened relative to traditional saw-tooth driving method.

Finally, the actuator excited by the SHDW, such as the symmetry of 50%, realizes a higher velocity and larger driving capacity relative to the asymmetrical hybrid driving waveform, such as the symmetries of 10%, 30%, 70%, and 90%. This paper may have some reference significance for the design and optimization of the symmetrical driving signals.

In addition, the hysteresis and the creeping property of the piezoelectric materials will be considered for establishing the stick-slip theory model of the actuator in future work.

REFERENCES

[1] T. Nishimura, H. Hosaka, and T. Morita, "Resonant-type smooth impact drive mechanism (SIDM) actuator using a bolt-clamped langevin transducer," *Ultrasonics*, vol. 52, no. 1, pp. 75–80, Jul. 2012.

[2] C. Meyer, O. Sqalli, H. Lorenz, and K. Karrai, "Slip-stick step-scanner for scanning probe microscopy," *Rev. Sci. Instrum.*, vol. 76, no. 6, pp. 063706-1–063706-5, May 2005.

[3] T. Morita, T. Nishimura, R. Yoshida, and H. Hosaka, "Resonant-type smooth impact drive mechanism actuator operating at lower input voltages," *Jpn. J. Appl. Phys.*, vol. 52, no. 7S, pp. 07HE05-1–07HE05-5, Jun. 2013.

[4] Y. Liu, D. Xu, X. Yang, and W. Chen, "Miniaturized piezoelectric actuator operating in bending hybrid modes," *Sens. Actuators A, Phys.*, vol. 235, no. 1, pp. 158–164, Nov. 2015.

[5] J. Li *et al.*, "Development of a novel parasitic-type piezoelectric actuator," *IEEE/ASME Trans. Mechatronics*, vol. 22, no. 1, pp. 541–550, Feb. 2016.

[6] M. Hunstig, "Piezoelectric inertia motors—A critical review of history, concepts, design, applications, and perspectives," *Actuators*, vol. 6, no. 1, pp. 1–35, Feb. 2017.

[7] Y. Liu, X. Yang, W. Chen, and D. Xu, "A bonded-type piezoelectric actuator using the first and second bending vibration modes," *IEEE Trans. Ind. Electron*, vol. 63, no. 3, pp. 1676–1683, Mar. 2016.

[8] C. Edeler, I. Meyer, and S. Fatikow, "Modeling of stick-slip micro-drives," *J. Micro-Nano Mech.*, vol. 6, nos. 3–4, pp. 65–87, Jun. 2011.

[9] M. Hunstig, T. Hemsel, and W. Sextro, "Stick–slip and slip–slip operation of piezoelectric inertia drives. Part I: Ideal excitation," *Sens. Actuators A, Phys.*, vol. 200, no. 4, pp. 90–100, Nov. 2013.

[10] T. Morita, H. Murakami, T. Yokose, and H. Hosaka, "A miniaturized resonant-type smooth impact drive mechanism actuator," *Sens. Actuators A, Phys.*, vol. 178, pp. 188–192, Feb. 2012.

[11] J. Lee, W. S. Kwon, K.-S. Kim, and S. Kim, "A novel smooth impact drive mechanism actuation method with dual-slider for a compact zoom lens system," *Rev. Sci. Instrum.*, vol. 82, no. 8, pp. 085105-1–085105-8, Aug. 2011.

[12] M. Hunstig, T. Hemsel, and W. Sextro, "Stick–slip and slip–slip operation of piezoelectric inertia drives—Part II: Frequency-limited excitation," *Sens. Actuators A, Phys.*, vol. 200, pp. 79–89, Oct. 2013.

[13] J. Li, X. W. Xiong, C. J. Liu, Y. F. Liu, and W. J. Zhang, "A computationally efficient model to capture the inertia of the piezoelectric stack in impact drive mechanism in the case of the in-pipe inspection application," *Mech. Sci.*, vol. 7, pp. 79–84, Mar. 2016.

[14] Z. M. Zhang, Q. An, J. W. Li, and W. J. Zhang, "Piezoelectric friction–inertia actuator—A critical review and future perspective," *Int. J. Adv. Manuf. Technol.*, vol. 62, nos. 5–8, pp. 669–685, Sep. 2012.

[15] C.-F. Yang, S.-L. Jeng, and W.-H. Chieng, "Motion behavior of triangular waveform excitation input in an operating impact drive mechanism," *Sens. Actuators A, Phys.*, vol. 166, no. 1, pp. 66–77, Mar. 2011.

[16] R. Yoshida, Y. Okamoto, and H. Okada, "Development of smooth impact drive mechanism (2nd report) optimization of waveform of driving voltage," *J. Jpn. Soc. Precis. Eng.*, vol. 68, no. 4, pp. 536–541, 2002.

[17] Y. Peng, J. Cao, Z. Guo, and H. Yu, "A linear actuator for precision positioning of dual objects," *Smart Mater. Struct.*, vol. 24, no. 12, pp. 125039-1–125039-9, Nov. 2015.

[18] Y. T. Ma, H. Shekhani, X. T. Yan, M. Choi, and K. Uchino, "Resonant-type inertial impact motor with rectangular pulse drive," *Sens. Actuators A, Phys.*, vol. 248, pp. 29–37, Jul. 2016.

[19] C. Renner, P. Niedermann, A. D. Kent, and O. Fischer, "A vertical piezoelectric inertial slider," *Rev. Sci. Instrum.*, vol. 61, no. 3, pp. 965–967, Mar. 1990.

[20] B. L. Blackford, M. H. Jericho, and M. G. Boudreau, "A vertical/horizontal two-dimensional piezoelectric driven inertial slider micropositioner for cryogenic applications," *Rev. Sci. Instrum.*, vol. 63, no. 4, pp. 2206–2209, Apr. 1992.

[21] K. Svensson, Y. Jompol, H. Olin, and E. Olsson, "Compact design of a transmission electron microscope-scanning tunneling microscope holder with three-dimensional coarse motion," *Rev. Sci. Instrum.*, vol. 74, no. 11, pp. 4945–4947, Nov. 2003.

[22] W. F. Smith, M. C. Abraham, J. M. Sloan, and M. Switkes, "Simple retrofittable long-range $x - y$ translation system for scanned probe microscopes," *Rev. Sci. Instrum.*, vol. 67, no. 10, pp. 3599–3604, Oct. 1996.

[23] J. Wang and Q. Lu, "How are the behaviors of piezoelectric inertial sliders interpreted?" *Rev. Sci. Instrum.*, vol. 83, no. 9, pp. 093701-1–093701-5, Sep. 2012.

[24] L. Wang, D. Chen, T. Cheng, P. He, X. Lu, and H. Zhao, "A friction regulation hybrid driving method for backward motion restraint of the smooth impact drive mechanism," *Smart Mater. Struct.*, vol. 25, no. 8, pp. 085033-1–085033-6, Jul. 2016.
[25] T. Cheng *et al.*, "Performance improvement of smooth impact drive mechanism at low voltage utilizing ultrasonic friction reduction," *Rev. Sci. Instrum.*, vol. 87, no. 8, p. 039608, Aug. 2016.
[26] T. Cheng, H. Li, M. He, H. Zhao, X. Lu, and H. Gao, "Investigation on driving characteristics of a piezoelectric stick–slip actuator based on resonant/off-resonant hybrid excitation," *Smart Mater. Struct.*, vol. 26, no. 3, pp. 035042-1–035042-2, Feb. 2017.
[27] J. Zheng, S. Takahashi, S. Yoshikawa, and K. Uchino, "Heat generation in multilayer piezoelectric actuators," *J. Amer. Ceram. Soc.*, vol. 79, no. 12, pp. 3193–3198, Dec. 1996.
[28] A. Ochi, S. Takahashi, and S. Tagam, "Temperature characteristics for multilayer piezoelectric ceramic actuator," *Jpn. J. Appl. Phys.*, vol. 24, pp. 209–212, Jan. 1985.

HENGYU LI was born in Jilin province, China, in 1991. He received the B.S. degree from the Changchun University of Technology, Changchun, China, in 2015, where he is currently pursuing the M.S. degree with the Department of Mechanical Engineering, Changchun University of Technology. His research interests include piezoelectric actuators and smart materials and structures.

YIKANG LI was born in Jilin province, China, in 1994. He received the B.S. degree from the Changchun University of Technology, Changchun, China, in 2017. He is currently pursuing the M.S. degree with the Department of Mechanical Engineering, Changchun University of Technology. His research interests include piezoelectric actuators and smart materials and structures.

TINGHAI CHENG was born in Heilongjiang province, China. He received the B.S. degree in mechanical design manufacturing and automation, the M.S. degree in mechanical design and theory, and the Ph.D. degree in the mechatronic engineering from the Harbin Institute of Technology, Harbin, China, in 2006, 2008, and 2013, respectively., He is currently an Associate Professor with the Department of Mechatronic Engineering, Changchun University of Technology, Changchun, China. His current research interests include piezoelectric actuators and piezoelectric energy harvesting.

XIAOHUI LU was born in Jilin province, China. She received the B.S. degree from Beihua University, the M.S. degree from the Lanzhou University of Technology, and the Ph.D. degree from Jilin University, Changchun, China, in 2004, 2007, and 2013, respectively. Her current research interests include vehicle powertrain control, model predictive control, and data-driven control.

HONGWEI ZHAO was born in Jilin province, China, in 1976. He received the Ph.D. degree in mechanical engineering from Jilin University, China, in 2006. In 2006, he was appointed as a Teacher with the College of Mechanical Science and Engineering, Jilin University, where he is currently a Professor. His current research is in the *in situ* test and the precision machinery.

HAIBO GAO was born in Heilongjiang province, China. He received the M.S. and Ph.D. degrees in mechanical engineering from the Harbin Institute of Technology (HIT), Harbin, China, in 1995 and 2003, respectively. He is currently a Professor and Vice Dean with the School of Mechatronics, HIT, and also the Vice Dean with the State Key Laboratory of Robotics and System of HIT. His research interests mainly focus on mobile robots, aerospace mechanism and control, and multi-legged robots.